Science of the Total Environment 927 (2024) 172278

Contents lists available at ScienceDirect

Science of the Total Environment

journal homepage: www.elsevier.com/locate/scitotenv

A quanta-independent approach for the assessment of strategies to reduce the risk of airborne infection

Amar Aganovic [a,*], Jarek Kurnitski [b,d], Pawel Wargocki [c]

[a] Department of Automation and Process Engineering, UiT The Arctic University of Norway, Tromsø, Norway
[b] Department of Civil Engineering and Architecture, Tallinn University of Technology, Tallinn, Estonia
[c] Department of Environmental and Resource Engineering, Technical University of Denmark, Copenhagen, Denmark
[d] Department of Civil Engineering, Aalto university, Espoo, Finland

HIGHLIGHTS

- A novel method independent of quanta load variations for any given virus is proposed.
- Determining local extremes of the Wells-Riley function allows comparing infection risk.
- Only input required is the removal rates before and after implementing measures.
- The application is demonstrated for different viruses and infection control methods.

GRAPHICAL ABSTRACT

A quanta-independent approach

The maximum absolute infection risk difference (%) between two scenarios with different removal mechanisms $\sum\lambda_1$ and $\sum\lambda_2$:

$$\Delta P_{abs.max} = 100 \cdot \left(e^{-a\cdot\frac{\ln\left(\frac{b}{a}\right)}{b-a}} - e^{-b\cdot\frac{\ln\left(\frac{b}{a}\right)}{b-a}} \right)$$

Non-steady-state solutions:

$$a = \frac{IR}{V\cdot\sum\lambda_2}\cdot\left(t + \frac{e^{-\sum\lambda_2\cdot t}-1}{\sum\lambda_2}\right) \quad \& \; b = \frac{IR}{V\cdot\sum\lambda_1}\cdot\left(t + \frac{e^{-\sum\lambda_1\cdot t}-1}{\sum\lambda_1}\right)$$

Steady state solutions:

$$a = \frac{IR\cdot t}{V\cdot\sum\lambda_2} \; \& \; b = \frac{IR\cdot t}{V\cdot\sum\lambda_1}$$

IR – inhalation rate $\left(\frac{m^3}{h}\right)$; V – room volume (m^3); t- exposure time (h)

ARTICLE INFO

Editor: Pavlos Kassomenos

Keywords:
Infection risk
Airborne transmission
Wells-Riley model
Respiratory virus

ABSTRACT

The Wells-Riley model is extensively used for retrospective and prospective modelling of the risk of airborne transmission of infection in indoor spaces. It is also used when examining the efficacy of various removal and deactivation methods for airborne infectious aerosols in the indoor environment, which is crucial when selecting the most effective infection control technologies. The problem is that the large variation in viral load between individuals makes the Wells-Riley model output very sensitive to the input parameters and may yield a flawed prediction of risk. The absolute infection risk estimated with this model can range from nearly 0 % to 100 % depending on the viral load, even when all other factors, such as removal mechanisms and room geometry, remain unchanged. We therefore propose a novel method that removes this sensitivity to viral load. We define a quanta-independent maximum absolute before-after difference in infection risk that is independent of quanta factors like viral load, physical activity, or the dose-response relationships. The input data needed for a non-steady-state calculation are just the removal rates, room volume, and occupancy duration. Under steady-state conditions the approach provides an elegant solution that is only dependent on removal mechanisms before

* Corresponding author.
E-mail address: amar.aganovic@uit.no (A. Aganovic).

https://doi.org/10.1016/j.scitotenv.2024.172278
Received 30 January 2024; Received in revised form 2 April 2024; Accepted 4 April 2024
Available online 5 April 2024

and after applying infection control measures. We applied this method to compare the impact of relative humidity, ventilation rate and its effectiveness, filtering efficiency, and the use of ultraviolet germicidal irradiation on the infection risk. The results demonstrate that the method provides a comprehensive understanding of the impact of infection control strategies on the risk of airborne infection, enabling rational decisions to be made regarding the most effective strategies in a specific context. The proposed method thus provides a practical tool for mitigation of airborne infection risk.

Nomenclature

C	CO_2 concentration in the space $[ppm]$
c_i	the quanta-response relationship $\left[\frac{quanta}{RNA}\right]$
c_v	viral load in the respiratory tract $\left[\frac{RNA}{mL}\right]$
C_0	CO_2 concentration in the outdoor air $[ppm]$
$\Delta P_{abs.}$	maximum absolute infection risk difference [%]
G_p	CO_2 generation per person $\left[\frac{L}{persons \bullet min}\right]$
IR	inhalation rate $\left[\frac{m^3}{h}\right]$
λ_{dec}	biological decay rate $\left[\frac{1}{h}\right]$
λ_{dep}	gravitational deposition rate $\left[\frac{1}{h}\right]$
λ_{vent}	ventilation rate $\left[\frac{1}{h}\right]$
$\sum \lambda_n$	sum of total removal rates $\left[\frac{1}{h}\right]$
N	inhaled dose of fictious quantas $[quanta]$
$n(t)$	quanta concentration at time t $\left[\frac{quanta}{m^3}\right]$
n_p	number of persons in the space [–]
S	quanta emission source rate $\left[\frac{quanta}{h}\right]$
S_{CO_2}	CO_2 emission rate $[ppm]$
t	exposure time $[h]$
V	room volume $\left[m^3\right]$
V_{exh}	the total volume of respiratory fluid exhaled per unit of time, $\left[\frac{ml}{h}\right]$

1. Introduction

1.1. Airborne infection control strategies in the built environment

The main lesson from the COVID-19 pandemic is that the very real risk of even more lethal and infective respiratory viruses that may occur in the future makes it imperative to develop protocols for the reduction of cross-infection in indoor environments (Morens et al., 2023; Hodson, 2022). Effective infection control and prevention strategies must be developed. Additionally, because the primary route for cross-infection has been found to be airborne transmission (Tan et al., 2023; Rayegan et al., 2023), the focus should be on the solutions and technologies that specifically reduce airborne transmission. Airborne transmission is understood as the transmission of diseases caused by the direct inhalation of virus-carrying respiratory droplets and/or aerosols which can vary in size, small aerosols remaining suspended in the air for extended periods (Wang et al., 2021). Depending on the airflow field, such aerosols can potentially travel distances longer than 1 to 2 m away from the infected individual(s) (Xie et al., 2007; Bourouiba et al., 2014). Combined with a relatively slow virus inactivation rate (Dabisch et al., 2021), the airborne route of transmission of infectious aerosols can therefore create a significant health risk throughout an entire indoor volume.

Even before airborne transmission was acknowledged by the World Health Organization (WHO) as the major mode of SARS-COV-2 spread (Lewis, 2022), we had seen a re-emergence of airflow supply and distribution methods as the preferred engineering means for controlling airborne infection. Supplying clean outdoor air, highly efficient filtration of recirculated air and installing portable air cleaners have all been considered as effective methods for reducing cross-infection because they remove or dilute virus-laden aerosols and droplets. Deactivation methods for aerosolized viruses have also been considered. They comprise adjusting air temperature and relative humidity (RH) (Dabisch et al., 2021) and using ultraviolet (UV) light (Biasin et al., 2021). As a result of new research (Luo et al., 2023), lowering the pH value of the air is now additionally being considered for virus deactivation.

Numerical studies using validated computational fluid dynamic (CFD) simulations have demonstrated that higher ventilation rates dilute infectious aerosols and reduce the risk of cross-infection (Motamedi et al., 2022; Mariam et al., 2021). WHO recommends ventilation rates corresponding to at least 10 L/s per person in buildings (WHO, 2021). In May 2023, the US Center for Disease Control and Prevention (CDC) announced recommendations regarding ventilation rate aimed at reducing indoor transmission of the SARS-CoV-2 virus and set the rate at 5 air changes per hour (h-1) (Furlow, 2023). They were subsequently followed by the American Society of Heating, Refrigerating and Air-Conditioning Engineers (ASHRAE) who published Standard 241 in which equivalent outdoor air supply rates for infection control are prescribed for different types of spaces, to ensure a low risk of cross-infection (ASHRAE Standard 241, 2023). In addition to that, other guidelines for post-COVID target ventilation rates have been issued by the Federation of European Heating, Ventilation and Air Conditioning Associations (REHVA) (Nordic Ventilation Group, 2022) and the Lancet COVID-19 Commission (The Lancet COVID-19 Commission Task Force on Safe Work, Safe School, and Safe Travel, 2023). The effective use of ventilation requires not only the definition of airflow rates but also of proper air distribution that ensures high ventilation efficiency (Izadyar and Miller, 2022); this issue is among others addressed by Standard 241 (ASHRAE Standard 241, 2023). This standard and other documents provide additional recommendations on the use of air purifiers, ultraviolet light and/or the filtration of recirculated air to achieve reduced cross-infection (WHO, 2021; ASHRAE Standard 241, 2023; The Lancet COVID-19 Commission Task Force on Safe Work, Safe School, and Safe Travel, 2023).

The effective use of the control strategies mentioned must be shown to reduce the risk of cross-infection. To achieve this goal, a model is needed for risk estimation and evaluation, so that they can be compared in terms of how well they achieve this goal. The most frequently used model for this purpose is the Wells-Riley model (Sze To GN and Chao, 2010). The model is used to estimate the absolute risk of cross-infection when knowing in principle how much virus is emitted and what removal methods are being applied, including engineering control methods. Unfortunately, the Wells-Riley model is very sensitive to input parameters, particularly the viral load. Considering the large variation in the virus emitted by infected individuals even when they are engaged in the same physical and vocal activity, and the variability of the viral load that will lead to cross-infection, the model provides a very unreliable estimate of the absolute infection risk (P) because the same removal mechanism can provide different risk reduction in two identical building typologies. This drawback greatly reduces the ability of the model to identify the most effective solutions for reducing the risk of cross-infection. The variation in viral load can be substantial, potentially differing by several orders of magnitude. According to some studies, the calculated absolute infection risk using the Wells-Riley model can range from nearly 0 % to 100 % even when other factors such as removal

mechanisms and room geometry remain constant (Aganovic et al., 2021). As a result, estimates of the risk of cross-infection that use different assumptions regarding input variables, especially viral load, will lead to very different estimates of the absolute infection risk (Jones et al., n.d.), making it difficult to reliably compare the effectiveness of different engineering solutions.

In view of the above limitations of the Wells-Riley model, the primary purpose of the present work was to amend it by developing a method that would allow the model estimates to remain independent of assumptions regarding viral load. This amendment would enable the users of the model to avoid drawing flawed conclusions. To achieve this objective, a method is proposed in which the relative impact of different inactivation and infection control mechanisms over the entire range of source emission rates (viral loads) is calculated.

1.2. Theoretical (modelling) background

Almost all web-based tools for predicting airborne transmission risk in indoor environments during the COVID-19 pandemic used the Wells-Riley model (de Oliveira et al., 2021; Mikszewski et al., 2021a; Aganovic et al., 2023; Harmon and Lau, 2022; Chatoutsidou and Lazaridis, 2019; Peng et al., 2022) as a basis for calculations. The Wells-Riley model is based on a simple exponential dose-response model in the following form:

$$P = 1 - e^{-N}(\%) \tag{1}$$

where N is the inhaled dose of fictitious quantas of virus, where one quanta ($N = 1$) corresponds to the number of $TCID_{50}$ (50 % Tissue Culture Infectious Dose) doses which cause infection among $P = 1 - e^{-1} = 63.2$ % of susceptible individuals.

The airborne transmission of respiratory viruses in the form of aerosols over long distances makes it possible to represent the dynamics of quanta concentration using mass balance equations. Two main assumptions allow the calculation of the concentration of quanta in an indoor space using the mass balance equation: i) immediate dilution of the expelled virus from the source (the infected person); and ii) the uniform spatial distribution of virus-carrying aerosols. The time-dependent quanta concentration $n(t)$ in the air can then be determined by solving a non-steady-state first-order mass balance equation:

$$V \bullet \frac{dn(t)}{dt} = S - V \bullet n(t) \bullet \sum \lambda \Rightarrow n(t) = n_0 \bullet e^{-\sum \lambda \bullet t} + \frac{S}{V \bullet \sum \lambda} \bullet \left(1 - e^{-\sum \lambda \bullet t}\right) \tag{2}$$

given that the quanta removal mechanisms $\sum \lambda$ $\left[\frac{1}{h}\right]$ and the quanta emission source rate S $\left[\frac{quanta}{h}\right]$ are known. Furthermore, given the susceptible person's inhalation rate IR (m^3/h), the total number of quanta inhaled n in an exposure time t is ($n_0 = 0$) (Jones et al., 2021):

$$N = IR \bullet \int_0^t n(t)\, dt = IR \bullet \frac{S}{V \bullet \sum \lambda} \bullet \left(t + \frac{e^{-\sum \lambda \bullet t} - 1}{\sum \lambda}\right) \tag{3}$$

The final form of the mass-balance equation coupled with the exponential dose-response model, also known as the Wells-Riley equation, has the following form:

$$P = 1 - e^{-S \bullet \frac{IR}{V \bullet \sum \lambda} \bullet \left(t + \frac{e^{-\sum \lambda \bullet t} - 1}{\sum \lambda}\right)} (\%) \tag{4}$$

As we can see from Eq. (2) the airborne virus concentration within a space is dependent on the quanta emission rate S defined as:

$$S = c_v \bullet c_i \bullet V_{exh} \tag{5}$$

c_i – the quanta-response relationship is defined as the ratio between one infectious quantum and the infectious dose expressed in viral copies, i.e., the number of viral RNA copies required to infect at least 63.21 % of susceptible persons, $\left[\frac{quanta}{RNA}\right]$

The variation in the viral load presented as a probability density function based on a log-normal distribution is shown in Fig. 1 for different viruses).

The variability in the emission rate of virus depending on physical and vocal activity cannot be precisely estimated as it depends to a large extent on an individual and on his/her disease status. Because of this high variability, the calculated infection risk will have high output variation. This variation is shown in Fig. 2 for a simple case of a standing and speaking infected individual in a 150 m^3 room after 2 h of exposure. The figure shows that even though the total volume of respiratory fluid exhaled Vexh was assumed to be constant, which is unrealistic, the calculated risk ranged from 0 to 100 % in the case of SARS-CoV-2 and Adenovirus.

The quanta-response relationship c_i differs for various virus strains. During the COVID-19 pandemic, due to the lack of data for SARS-CoV-2, many of the papers based the quanta-viral copies relationship on the dose-response model for SARS-CoV-1developed by Watanabe et al. (Watanabe et al., 2010). Even though more data became available as the pandemic progressed (Aganovic and Kadric, 2023), the exact dose-response relationship for SARS-CoV-2 is still regarded as unknown.

These dose-response relationships are difficult to derive not only because of a lack of human challenge data but also because they vary between different virus variants. This means that the dose-response relationship, or more specifically the quanta-RNA copies relationship for the original SARS-CoV-2 Wuhan strain, is not the same as for the other variants of the SARS-CoV-2 virus. It follows that the infection risk will differ for other types of respiratory viruses. Consequently, a high infection risk due to exposure to a high spatial concentration of RNA copies of one virus strain does not necessarily translate to a high infection risk for another virus variant or type.

Taking the above into account, the present work proposes the use of the Wells-Riley equation for estimating the risk of cross-infection and thereby comparing infection control strategies independently of the quanta estimation rate parameters, namely c_v, c_i and V_{exh}. The approach compares how various removal methods relatively affect the absolute infection risk for constant source and room geometry conditions. This is done by comparing the absolute infection risks using Eq. (1) when increasing or decreasing the removal mechanism, while accounting for the diverse range of quanta estimation rates as shown in Fig. 3. This method makes it possible to compare different ventilation rates or virus inactivation methods, such as altering the room's relative humidity, or the influence of UV lighting for the same boundary conditions.

In simpler terms, the aim is to determine the maximum value of the

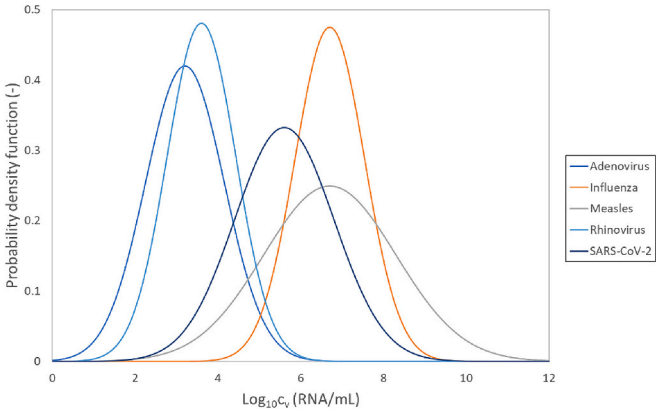

Fig. 1. The probability density function for an assumed log-normal distribution of the viral load c_v (RNA/Ml) (extracted from Iddon et al. (Iddon et al., 2022)) for certain airborne respiratory viruses (extracted from Iddon et al. (Iddon et al., 2022)).

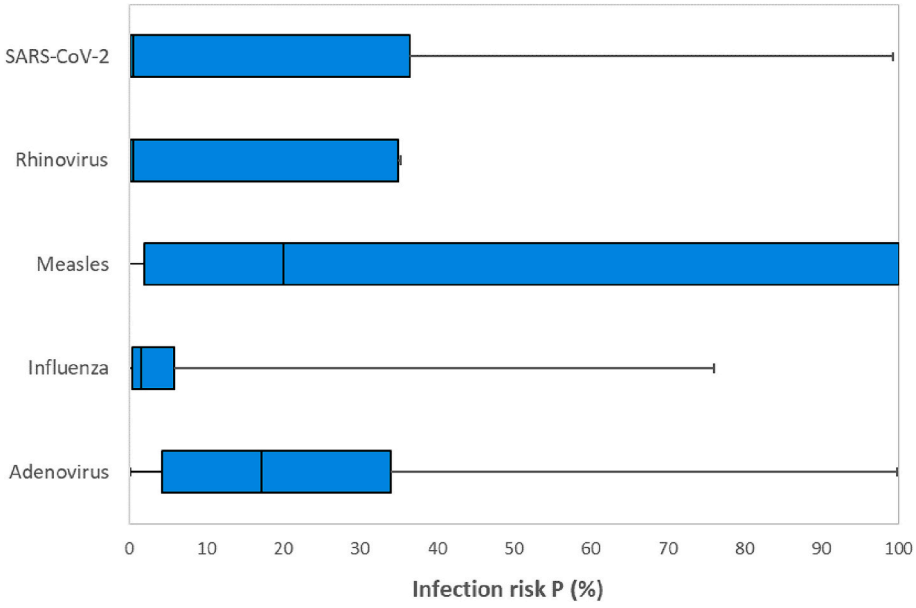

Fig. 2. Infection risk P (%) distributions for standing and speaking infected individuals in a 150 m^3 room after 2 h of exposure. Boxes span the interquartile ranges, while whiskers depict the 1st-99th percentile outliers and the 50th percentile denoted by the vertical line in each box. The infection risk variations are due only to variations in the viral load c_v, as V_{exh} and c_i were kept constant.

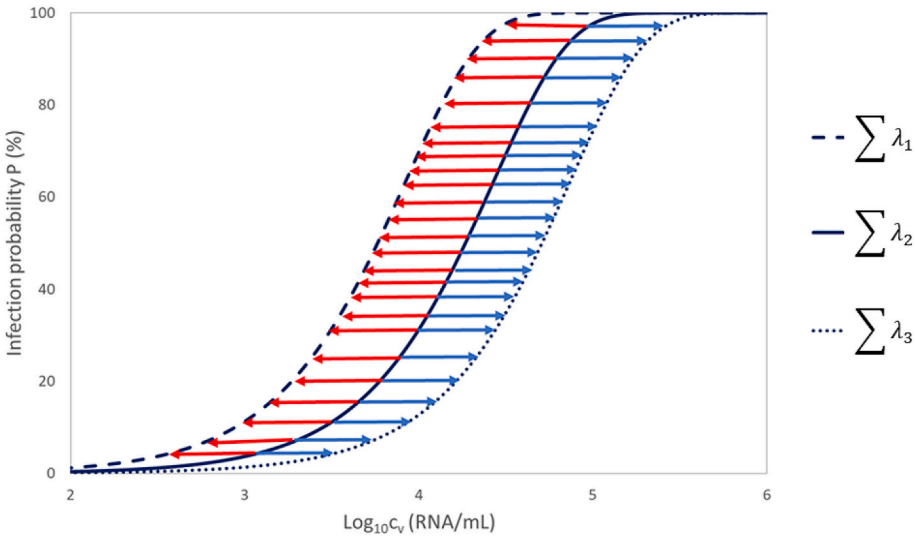

Fig. 3. The change in the infection risk distribution P(%) as a function of viral load c_v when changing the total removal mechanism$\sum\lambda_n$. Increasing $\sum\lambda_n$ is depicted by blue arrow lines, while decreasing $\sum\lambda_n$ is shown by red arrow lines.

absolute difference function $\Delta P_{abs.max} = 100\% \bullet \left| P_{\sum\lambda_2} - P_{\sum\lambda_1} \right|$ for the quanta estimation rate range $S_{min} \le S \le S_{max}$.

2. Methods

The time-dependent quanta concentration n(t) can be solved using the non-steady-state mass balance Eq. (2) in a room of volume V and at a certain time interval *t*. The quanta removal mechanism from Eq. (2) can be simplified as follows:

$$\sum\lambda = \lambda_{vent} + \lambda_{dep} + \lambda_{dec} \tag{6}$$

For a given quanta emission rate *S*, the absolute infection risk difference when changing the removal mechanism rate from $\sum\lambda_1$ to $\sum\lambda_2$ is then given by:

$$\Delta P_{abs.} = P_1 - P_2 = e^{-S\bullet\frac{IR}{V\bullet\sum\lambda_2}\bullet\left(t+\frac{e^{-\sum\lambda_2\bullet t}-1}{\sum\lambda_2}\right)} - e^{-S\bullet\frac{IR}{V\bullet\sum\lambda_1}\bullet\left(t+\frac{e^{-\sum\lambda_1\bullet t}-1}{\sum\lambda_1}\right)} \tag{7}$$

When planning the use of engineering control measures for airborne transmission risk, it is important to define the applicable range of the source rates considered. This range can be determined by calculating the local extremes of the source function, Eq. (5), defining quanta emission rate or viral load. We thus need to define the maximum of the $\Delta P_{abs.max}$ as a function of the quanta emission rate *S*. To do so, the function $\Delta P_{abs.}$, Eq. (7), can be defined as follows:

$$\Delta P_{abs.} = f_1(S) = e^{-a\bullet S} - e^{-b\bullet S},$$

where the source rate range is defined as follows:

$S_{min} \le S \le S_{max}$ and $> 0 \& b > 0 \& a < b$.

The local maximum can be found by solving for the following derivative:

$$f_1'(S) = -a \bullet e^{-a \bullet S} + b \bullet e^{-b \bullet S} = 0$$

This yields a solution that $f_1(S)$ will reach its extreme value for $S_{extreme} = \frac{ln\left(\frac{b}{a}\right)}{b-a}$.

The local minimum can be then defined for the lower value of $f_1(S_{min})$ *or* $f_1(S_{max})$.

If $min(\Delta P_{abs.}(S_{min}), \Delta P_{abs.}(S_{max})) \rightarrow 0\%$then the absolute change in cross-infection risk will have the following range (as illustrated in Fig. 4):

$$0\% < \Delta P_{abs.}(S) \le \Delta P_{abs.}\left(\frac{ln\left(\frac{b}{a}\right)}{b-a}\right) \quad (8)$$

In other words, the maximum absolute difference between two scenarios with different removal mechanisms will occur for:

$$\Delta P_{abs.max} = \Delta P_{abs.}\left(\frac{ln\left(\frac{b}{a}\right)}{b-a}\right) \quad (9)$$

where for the non-steady-state solutions:

$$a = \frac{IR}{V \bullet \sum \lambda_2} \bullet \left(t + \frac{e^{-\sum \lambda_2 \bullet t} - 1}{\sum \lambda_2}\right) \quad (10)$$

$$b = \frac{IR}{V \bullet \sum \lambda_1} \bullet \left(t + \frac{e^{-\sum \lambda_1 \bullet t} - 1}{\sum \lambda_1}\right) \quad (11)$$

and for the steady-state solutions:

$$a = \frac{IR \bullet t}{V \bullet \sum \lambda_2} \quad (12)$$

$$b = \frac{IR \bullet t}{V \bullet \sum \lambda_1} \quad (13)$$

Inserting a and b into $\Delta P_{abs.} = e^{-a \bullet S} - e^{-b \bullet S}$ results in a solution which has the following form for the steady-state condition:

$$\Delta P_{abs.max} = e^{-\frac{\sum \lambda_1 ln \frac{\sum \lambda_2}{\sum \lambda_1}}{\sum \lambda_2 - \sum \lambda_1}} - e^{-\frac{\sum \lambda_2 ln \frac{\sum \lambda_2}{\sum \lambda_1}}{\sum \lambda_2 - \sum \lambda_1}} \quad (14)$$

If $\Delta P_{abs.max} > 0$ then there is a relative decrease in infection risk after applying infection risk measures.

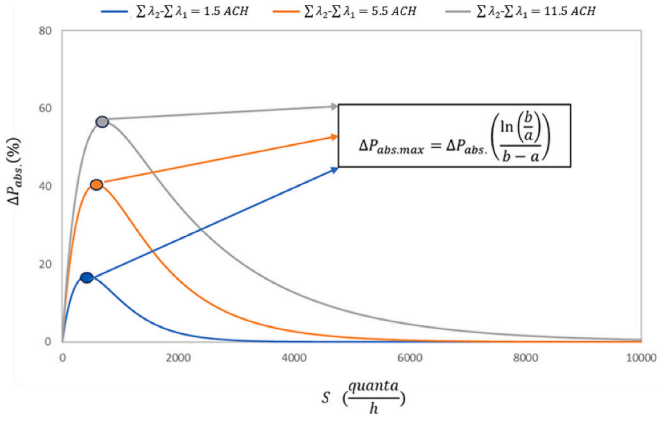

Fig. 4. An example of how to determine the maximum absolute difference for the exponential (Wells-Riley) infection risk probability.

The $S_{extreme}$ for steady-state conditions can be back-calculated as

$$S_{extreme} = -ln\left(1 - e^{-\frac{\lambda_2 ln \frac{\lambda_2}{\lambda_1}}{\lambda_2 - \lambda_1}}\right) \bullet V \bullet \lambda_1 \quad (15)$$

or

$$S_{extreme} = -ln\left(1 - e^{-\frac{\lambda_1 ln \frac{\lambda_2}{\lambda_1}}{\lambda_2 - \lambda_1}}\right) \bullet V \bullet \lambda_2 \quad (16)$$

Eq. (9) should be used with caution because $S_{extreme} = \frac{ln\left(\frac{b}{a}\right)}{b-a}$ may be outside the range for quanta estimation outliers for a given virus (Mikszewski et al., 2021b). In the present method, the range will be defined by the 99th percentile of the range for the quanta estimation rates based on a normal distribution of the viral load c_v as provided by Mikszewski et al. (Mikszewski et al., 2021b) and as shown in Table 1. So, $S_{min} = 0\%$(no infected persons present) and $S_{max} = S_{99\%}$.

If the $S_{extreme} = \frac{ln\left(\frac{b}{a}\right)}{b-a}$ lies outside the range defined by the the 99th percentile ($S_{99\%}$) then the absolute difference can be defined as follows:

If $\frac{ln\left(\frac{b}{a}\right)}{b-a} > S_{99\%}$ then $\Delta P_{abs.max} = \Delta P_{abs.}(S_{99\%})$.

The main reason we chose the absolute difference $100\% \bullet \left|P_{\sum \lambda_2} - P_{\sum \lambda_1}\right|$ rather than the relative difference $100\% \bullet \left|\frac{P_{\sum \lambda_2} - P_{\sum \lambda_1}}{P_{\sum \lambda_1}}\right|$ is that the absolute difference is specific only for one quanta value while the relative is not. Decreasing the infection risk from 50 % to 10 % and from 0.05 % to 0.01 % for different source input values will result in the same relative decrease of 80 %, but the absolute difference will differ substantially, by 40 % and 0.04 % respectively. In other words, the absolute comparison is a better representation of reducing the maximum potential airborne infection threat than the relative comparison.

In the proposed methodology, the gravitational deposition rate was approximated at $\lambda_{dep} = 0.24\ h^{-1}$ (Chatoutsidou and Lazaridis, 2019) while the biological decay (h^{-1}) was assumed to depend on the virus type and variant and indoor environmental conditions including relative humidity and temperature. Assuming that relative humidity has a negligible effect on the size change and thus on the deposition rate of aerosols in the range of 20 % to 70 % (Aganovic et al., 2022a), then any relative changes in quanta concentrations for a given quanta/viral load source will depend only on changes in ventilation rate λ_{vent} and/or the biological decay rate, λ_{dec}, ventilation being an engineering infection control measure. Removal by ventilation can be based on recent recommendations (WHO, 2021; Furlow, 2023; ASHRAE Standard 241, 2023; Nordic Ventilation Group, 2022; The Lancet COVID-19 Commission Task Force on Safe Work, Safe School, and Safe Travel, 2023). It can also be proxied by the CO_2 mass balance model but the same boundary and time-step conditions as used for the quanta mass balance model must be used. The concentration of CO_2 above background level ($\Delta C = C - C_0$) and virus concentration in air $n(t)$ can be solved using the non-steady-state mass balance equation taking the same room volume V (as

Table 1

The 50th ($S_{50\%}$), and 99th ($S_{99\%}$) percentile of quanta emission rates S $[\frac{quanta}{h}]$ as a function of the expiratory activity and activity level, presented in the table as $S_{50\%}$ $[S_{99\%}]$.

Virus	Resting, oral breathing	Standing, Speaking	Light activity, speaking loudly
Adenovirus	0.78 [126]	3.9 [629.79]	66.0 [$1.07 \bullet 10^4$]
Influenza	0.035 [3.15]	0.17 [15.69]	3.0 [265.74]
Measles	3.1 [$1.64 \bullet 10^4$]	15 [$8.17 \bullet 10^4$]	260 [$1.38 \bullet 10^6$]
Rhinovirus	0.21 [17.70]	1.0 [88.17]	18 [1493.56]
SARS-CoV-2	0.55 [339.42]	2.7 [1690]	46 [$2.86 \bullet 10^4$]

for the quanta mass balance) and identical time. Then the ventilation removal mechanism can be defined as $\lambda_{vent} = \lambda_{vent-CO_2} = \frac{\dot{V}}{V}$ where $\dot{V}$ is the virus-free supply airflow rate to the room (m^3/h) needed to reach the desired CO_2 level (corresponding to the effect obtained by ventilation with outdoor air) using the non-steady-state mass balance equation as follows:

$$V \bullet \frac{d\Delta C(t)}{dt} = S_{CO_2} - V \bullet \Delta C(t) \bullet \sum \lambda_{CO_2} => \Delta C(t) = \Delta C_0 \bullet e^{-\sum \lambda_{vent-CO_2} \bullet t} + \frac{S_{CO_2}}{V \bullet \sum \lambda_{CO_2}} \bullet \left(1 - e^{-\sum \lambda_{vent-CO_2} \bullet t}\right) \quad (17)$$

Where $\Delta C = C - C_0$ is the difference between the CO_2 concentration in the space C (ppm) and C_0 is the background concentration. Further, the CO_2 source rate S_{CO_2} in Eq. (2) can be calculated as:

$$S_{CO_2} = n_p \bullet G_p \quad (18)$$

The only parameter is the age- and activity-level-specific G_p and this can be calculated according to Battermann as a function of metabolic rate (activity level) and skin area (Batterman, 2017); these equations are omitted in the present paper and can be found in Battermann et al. (Batterman, 2017). In the case when the room was initially unoccupied, i.e., $n_0 = 0$ and $\Delta C_0 = 0$, Eq. (2) becomes:

$$n(t) = \frac{S_n}{V \bullet \left(\lambda_{vent-CO_2} + \lambda_{dep} + \lambda_{dec}\right)} \bullet \left(1 - e^{-\left(\lambda_{vent-CO_2} + \lambda_{dep} + \lambda_{dec}\right) \bullet t}\right) \quad (19)$$

3. Results

An application of the proposed methodology will now be described. It is assumed that by using infection control measures the total removal rate increases from $\sum \lambda_1 = 2.0\ h^{-1}$ to $\sum \lambda_2 = 4.0\ h^{-1}$; for simplification it is assumed that the total removal rate is the same for all viruses in the room volume of V = 150 m^3. The infection risk and the absolute difference in the infection risk is calculated for the 1st, 5th, 50th, 95th, and 99.9th percentile of quanta emission rates for steady-state conditions in the case of the following respiratory viruses: (i) Adenovirus; (ii) Influenza; (iii) Measles; (iv) Rhinovirus; and (v) SARS-CoV-2. The quanta emission rate for each virus at different confidence intervals is derived from Mikszewski et al. (Mikszewski et al., 2021b) and Aganovic et al. (Aganovic et al., 2023). By using the difference between the absolute values$\Delta P_{abs} = P_1 - P_2$ calculated by using Eq. (4) and the $\Delta P_{abs.max}$ calculated for steady state using Eq. (9), the difference in infection risks before (at a removal rate of 2 h^{-1}) and after (at a removal rate of 4 h^{-1}) taking the infection control measure are calculated and shown in Table 2:

In the example presented in Table 2 we show that by deriving the absolute infection risk difference $0 < \Delta P_{abs.} \leq 25.0\%$ using Eq. (9) we narrow down the range of possibilities for reducing infection risk when considering different inactivation mechanisms. In other words, the maximum absolute probability decrease that can be achieved by increasing the removal rate from 2.0 to 4.0 ACH is 25.0 % for a quanta rate of 415.8 $\frac{quanta}{h}$.; the removal rate can also be the deactivation rate corresponding to the effects defined by the removal rate range.

Table 2 shows that absolute difference varies for different virus types and quanta percentile values. It shows that even for the wide range of quanta rate conditions, the maximum absolute infection risk will be the same for all viruses, as defined by $\Delta P_{abs.max}$, and will not be higher than the maximum (in Table 2 the maximum difference in the risk infection was 24.9 % for different quanta which is lower than the maximum absolute risk difference). The proposed absolute infection risk difference thus allows accurate estimation of the range of the effect on the infection risk when comparing two removal mechanisms. The approach illustrated in Table 2 is independent of the person's activity, viral load, or even virus strain.

The application of the methodology can also be demonstrated by comparing different infection control measures in a hypothetical classroom. These measures include: (i) relative humidity; (ii) ventilation rate; (iii) ventilation effectiveness; (iv) filtration efficiency of recirculated air (100 % recirculation); and (v) upper room ultraviolet germicidal irradiation (UVGI). The same room is considered as in the previous scenario (V = 150 m3) but different inactivation rates λ_{dec} are considered for the various viruses based on the data derived from experimental studies (Aganovic et al., 2022b). The five measures listed ($\sum \lambda_2$) are compared to the reference scenario ($\sum \lambda_1$) using $\Delta P_{abs.max}$, i.e., Eq. (9) for steady state conditions. The reference scenario is RH = 50–55 % for all considered viruses except for Measles (RH = 68–70 %), a ventilation rate of 0.5 h^1 except for the relative humidity and UVGI when the ventilation rate is set to keep the CO_2 concentration ≤ 1000 ppm ($\lambda_{vent} = 2.87\ h^{-1}$), ventilation effectiveness $\varepsilon_v = 1$ with no recirculation and no UVGI. In the case of recirculation, a MERV 5 filter is assumed in the reference scenario. The $\Delta P_{abs.max}$ for the five measures are shown in Table 3.

The absolute $\Delta P_{abs.max}$ shows the opportunities and limits when implementing the specific infection control measure. It depends on the virus types and they have different inactivation rates.

In the case of RH, humidification may decrease the cross-infection risk by up to 8.3 % for influenza and up to 5.4 % for SARS-CoV-2, while increase the absolute difference risk for up to 66.32 % for rhinovirus and almost 11 % for adenovirus, which is similar to what has been observed before (Aganovic et al., 2021; Aganovic et al., 2022a). The effect on immunological response of changing RH is not considered here.

Ventilation decreases the risk regardless of the virus type. The relative impact depends on the inactivation rate of the virus considered: the highest impact can be observed for SARS-CoV-2 ($\lambda_{dec} = 0.48\ h^{-1}$) and the lowest for Rhinovirus ($\lambda_{dec} = 23.96\ h^{-1}$). It is interesting to note that although the differences between the assumed inactivation rates for SARS-CoV-2 and Influenza are almost negligible ($\lambda_{dec} = 0.485\ h^{-1}$), the calculated value $\frac{ln\left(\frac{b}{a}\right)}{b-a} > S_{99\%}$ for Influenza so $\Delta P_{abs.}(S_{99\%})$ was used rather than $\Delta P_{abs.}\left(\frac{ln\left(\frac{b}{a}\right)}{b-a}\right)$, resulting in lower maximum absolute differences for

Table 2
The absolute difference in infection risk $\Delta P_{abs} = P_1 - P_2$ (S) by changing the removal rate from 2 h^{-1} to 4 h^{-1}. S is the quanta emission rate (quanta/h)

Virus	$\Delta P_{abs} = P_1 - P_2$ (S) (Eq. (4))					$\Delta P_{abs.max}$ (S_{max}) (Eq. (9))
	0.1 %	5 %	50 %	95 %	99.9 %	
Adenovirus	<0.0 % ($8.0 \bullet 10^{-2}$)	−0.3 % (1.8)	−9.3 % (66.0)	−1.8 % (2400.0)	<0.0 % ($5.7 \bullet 10^{4}$)	−25.0 % (415.8)
Influenza	<0.0 % ($8.2 \bullet 10^{-3}$)	<0.0 % (0.1)	−0.5 % (3.0)	−10.0 % (72.0)	−12.3 % (1164.5)	
Measles	<0.0 % ($3.0 \bullet 10^{-3}$)	−0.1 % (0.6)	−22.8 % (260.0)	<0.0 % ($1.1 \bullet 10^{5}$)	<0.0 % ($5.7 \bullet 10^{7}$)	
Rhinovirus	<0.0 % (0.0)	−0.1 % (0.8)	−2.9 % (18.0)	−24.9 % (420.0)	<0.0 % ($6.4 \bullet 10^{3}$)	
SARS-CoV-2	<0.0 % ($9.1 \bullet 10^{-3}$)	<0.0 % ($2.0 \bullet 10^{-2}$)	−0.4 % (2.4)	−21.4 % (222.2)	<0.0 % ($1.2 \bullet 10^{4}$)	

Influenza.

Increasing and decreasing ventilation effectiveness is shown to have effects similar to those of ventilation rate but results in different magnitude of the effects for different viruses. Improving ventilation effectiveness is shown to reduce the risk while decreasing ventilation effectiveness is predicted to considerably increase the infection risk for SARS-COV-2, Influenza, and Adenovirus.

We also calculated $\Delta P_{abs.max}$ when implementing increasing ventilation rate, ventilation efficiency, filtration, and UVGI irradiation at the same time. Table 3 shows that the absolute effects are not additive. Adding one more strategy will decrease the absolute risk $\Delta P_{abs.max}$ but the combined effect of different measures was lower than the sum $\Delta P_{abs.max}$ of the reductions obtained by taking each measure individually.

4. Discussion

Throughout the last pandemic, the risk of infection was estimated mainly using the Wells-Riley model for airborne infection. For instance, Kurnitski et al. (Kurnitski et al., 2023) proposed a ventilation design method based on quanta emission rate at median viral load, allowing the calculated target ventilation rate to be a function of the number of occupants, room volume, and ventilation effectiveness. However, this approach, which combines a mass balance equation with the concept of quanta in the Wells-Riley model, depends on the assumptions regarding quanta emission rate which is highly influenced by an infected person's viral load and physical activity, which may vary by several orders of magnitude. This variation can be the source of bias and serious error. Consequently, the variability in viral loads among individuals and across different respiratory viruses, coupled with the variability between individuals in terms of their physical activities, introduces a significant fragility to the Wells-Riley model. The resulting infection risk output is highly sensitive to the input conditions, which can result in a broad range of calculated risks even when other environmental parameters remain unchanged. Application of the Wells-Riley model can easily bias estimation of effectiveness when comparing different control measures effectiveness at a fixed quanta emission rate.

While our method builds upon prior research in quanta-independent infection risk modelling, including the work of Jones et al. (Jones et al., 2021) and Peng and Jimenez (Peng and Jimenez, 2021), we propose an alternative approach to address a specific limitation of the Wells-Riley model. Previous research has indeed considered relative infection risk assessment (percentage change) independent of quanta estimation rates under steady-state assumptions and assuming that the infection risk equals the quanta concentration, as highlighted by Jones et al. (Jones et al., n.d.) and Iddon et al. (Iddon et al., 2022). The novelty of our approach is that we do not rely on these assumptions. Instead, we introduce the concept of absolute difference risk (percentage-point changes), which is valid for both steady-state and non-steady-state solutions, and assume the infection risk can be calculated using the exponential Wells-Riley model.

The proposed method is summarized in Fig. 5; it is independent of variables such as viral load, droplet emission rate, and physical activity.

In the proposed method, a reference scenario of the worst possible removal rate, i.e., low ventilation rate and effectiveness, no other removal mechanisms, can be established for the rooms in question. By applying infection risk control measures for the reference scenario, it is easy to calculate how much the infection risk can be reduced and to select the most effective measures. Input data needed for this calculation are just the removal rates, room volume, and occupancy duration. Furthermore, the steady-state condition results in a more elegant solution, dependent only on removal mechanisms before ($\sum \lambda_1$) and after ($\sum \lambda_2$) applying the infection control measures:

$$\Delta P_{abs.max} = e^{-\frac{\sum \lambda_1 ln\frac{\sum \lambda_2}{\sum \lambda_1}}{\sum \lambda_2 - \sum \lambda_1}} - e^{-\frac{\sum \lambda_2 ln\frac{\sum \lambda_2}{\sum \lambda_1}}{\sum \lambda_2 - \lambda_1}}$$

Table 3
$\Delta P_{abs.max}$ calculated using Eq. (9) for various engineering infection control strategies for five different airborne viruses at the steady state conditions. (+) = relative increase in infection risk & (−) = relative decrease in infection risk.

	$\Delta P_{abs.max}$ (Eq. (9))				
	SARS-CoV-2	Influenza	Rhinovirus	Measles	Adenovirus
Relative humidity (RH) [34][a]					
Increasing RH 50 % → 65 %	N/A	−8.3 %	N/A	N/A	N/A
Increasing RH 50 % → 70 %	−5.4 %	N/A	N/A	N/A	N/A
Increasing RH 50 % → 80 %	N/A	N/A	+ 66.3 %	N/A	+10.9 %
Decreasing RH 50 % → 30 %	N/A	N/A	≈0.0 %	N/A	N/A
Decreasing RH 50 % → 20 %	−1.2 %	+3.6 %	N/A	N/A	+0.9 %
Ventilation (outdoor air)[b]					
Increasing 0.5 h^{-1} → 2.0 h^{-1}	−28.7 %	−28.7 %	−2.2 %	−6.0 %	−17.2 %
Increasing 2.0 h^{-1} → 6.0 h^{-1}	−32.1 %	−24.6 %	−5.2 %	−12.3 %	−25.1 %
Increasing 0.5 h^{-1} → 6.0 h^{-1}	−56.0 %	−53.4 %	−7.4 %	−18.2 %	−40.7 %
Ventilation effectiveness[c]					
Decreasing ε_v = 1.0 → 0.3 (2.0 h^{-1})	+ 25.9 %	+ 25.9 %	+ 2.0 %	+ 5.6 %	+ 15.6 %
Decreasing ε_v = 1.0 → 0.3 (6.0 h^{-1})	+ 34.4 %	+ 27.2 %	+ 5.5 %	+13.1 %	+ 26.8 %
Increasing ε_v = 1.0 → 2.0 (0.5 h^{-1})	−12.5 %	−12.3 %	−0.7 %	−2.1 %	−6.7 %
Increasing ε_v = 1.0 → 2.0 (2.0 h^{-1})	−19.8 %	−16.5 %	−2.7 %	−6.7 %	−14.8 %
Filtration efficiency (100 % recirculation)[a,d]					
MERV 5 → MERV 10	−21.0 %	−20.8 %	−1.4 %	−3.9 %	−11.9 %
MERV 10 → MERV 13	−15.6 %	−14.4 %	−1.6 %	−4.2 %	−10.6 %
MERV 5 → HEPA	−37.9 %	−37.6 %	−3.3 %	−9.0 %	−24.1 %
MERV 10 → HEPA	−18.2 %	−16.8 %	−2.0 %	−5.1 %	−12.6 %
MERV 13 → HEPA	−2.8 %	−2.3 %	−0.3 %	−0.9 %	−2.0 %
Upper room UVGI (Aganovic et al., 2023; McDevitt et al., 2010)[a,b,d]					
None → Low	−6.3 %	−4.9 %	−0.9 %	−2.2 %	−4.8 %
None → Medium	−11.7 %	−8.8 %	−1.8 %	−4.3 %	−9.0 %
None → High	−20.4 %	−14.4 %	−3.5 %	−8.2 %	−16.2 %
Combined measures					
Increasing 0.5 h^{-1} → 2.0 h^{-1} + Increasing ε_v = 1.0 → 2.0	−46.2 %	−45.2 %	−4.87 %	−12.65 %	−31.4 %
Increasing 2.0 h^{-1} → 6.0 h^{-1} + Increasing ε_v = 1.0 → 2.0	−51.7 %	−34.7 %	−11.8 %	−25.0 %	−43.8 %
Increasing 2.0 h^{-1} → 6.0 h^{-1} + Increasing ε_v = 1.0 → 2.0 +	−59.6 %	−57.8 %	−7.6 %	−18.9 %	−42.7 %

(continued on next page)

Table 3 (*continued*)

	$\Delta P_{abs.max}$ (Eq. (9))				
	SARS-CoV-2	Influenza	Rhinovirus	Measles	Adenovirus
MERV 5 → HEPA					
Increasing 2.0 h^{-1} → 6.0 h^{-1} + Increasing ε_v = 1.0 → 2.0 + UVGI (high)	−56.8 %	−36.9 %	−14.4 %	−29.4 %	−48.6 %

[a] Considered for the same classroom in Example 1 with the ventilation rate set to keep CO_2 concentration ≤ 1000 ppm, i.e., the ventilation rate is $\lambda_{vent} = 2.87$ h^{-1}.

[b] Inactivation rate is kept constant $\lambda_{dec} = 0.48$ h^{-1} for SARS-CoV-2, $\lambda_{dec} = 0.485$ h^{-1} for Influenza, $\lambda_{dec} = 23.96$ h^{-1} for rhinovirus and $\lambda_{dec} = 1.741$ h^{-1} for Adenovirus for the range RH = 50–55 % (Aganovic et al., 2022b) and $\lambda_{dec} = 7.736$ h^{-1} at RH = 68–70 %.

[c] Ventilation effectiveness $\varepsilon_v = 1$ at a constant ventilation rate (fully mixed conditions).

[d] Particle removal efficiency η_{filt} values used for filters: η_{MERV5}=17 %; η_{MERV10}=50 %; η_{MERV13}=90 %; η_{HEPA}=99.9 %. N/A -not available inactivation rates at given RH values. Based on different upper room susceptibility constant Z_{UP} (m^2/J) values (Aganovic et al., 2023), $\lambda_{UVGI,low} = 0.67$ h^{-1}, $\lambda_{UVGI,med} = 1.35$ h^{-1}, $\lambda_{UVGI,high} = 2.71$ h^{-1}.

A quanta-independent approach

The maximum absolute infection risk difference (%) between two scenarios with different removal mechanisms $\sum\lambda_1$ and $\sum\lambda_2$:

$$\Delta P_{abs.max} = 100 \cdot \left(e^{-a \cdot \frac{\ln\left(\frac{b}{a}\right)}{b-a}} - e^{-b \cdot \frac{\ln\left(\frac{b}{a}\right)}{b-a}} \right)$$

Non-steady-state solutions:

$$a = \frac{IR}{V \cdot \sum\lambda_2} \cdot \left(t + \frac{e^{-\sum\lambda_2 \cdot t} - 1}{\sum\lambda_2}\right) \quad \& \; b = \frac{IR}{V \cdot \sum\lambda_1} \cdot \left(t + \frac{e^{-\sum\lambda_1 \cdot t} - 1}{\sum\lambda_1}\right)$$

Steady state solutions:

$$a = \frac{IR \cdot t}{V \cdot \sum\lambda_2} \; \& \; b = \frac{IR \cdot t}{V \cdot \sum\lambda_1}$$

IR – inhalation rate $\left(\frac{m^3}{h}\right)$; V – room volume ($m^3$); t- exposure time (h)

Fig. 5. The method proposed in this paper that improves the application of the Wells-Riley infection risk model. The method defines the absolute difference independent of quanta emission rate and thus independent of viral load, physical activity and virus type.

The quanta-independent infection risk assessment method illustrated in Table 3 is expected to be a useful tool for public health, infection control and engineering experts who must compare the maximum effect of different mitigation strategies in terms of how well they reduce the airborne cross-infection risk.

It is also possible to use the Wells-Riley-based design approach (Kurnitski et al., 2023) to assess some measures whose effectiveness can be compared with a reference scenario using this new method. Therefore, the proposed quanta-independent approach can provide solid arguments, as it is based on the absolute difference, for the selection of relevant measures and can be applied together with quanta-based methods. Future research could investigate which emission rates interventions exert the most significant change and compare this range to the total possible emission rates. This analysis would reveal the proportion of emissions that fall within the optimal range for maximum impact of removal mechanisms. This aligns with the concept of the "goldilocks zone" discussed by Iddon et al. (Iddon et al., 2022), indicating the narrow window within which interventions are most successful.

It must be noted that all the limitations related to the Wells-Riley model assumptions still apply, as summarized in previous studies (Aganovic et al., 2021; Aganovic et al., 2022b). While our method focuses on overcoming uncertainty surrounding quanta emission rate estimation, it is important to acknowledge that the uncertainty of removal rates for biological and deposition processes was not explicitly considered in this study. In addition, our study primarily focuses on scenarios where one or more occupants are infected, as our method aims to address infection risk estimation in situations where viral transmission is possible. This focus allows for a clear demonstration of our method's applicability in scenarios with varying levels of infection prevalence. However, it is important to note that our method does not explicitly consider scenarios where no individuals are infected. Future research should aim to incorporate these additional sources of uncertainty in the model to provide a more comprehensive understanding of infection risk dynamics in indoor environments.

5. Conclusions

We proposed a method for calculating the impact of airborne infection control strategies in a shared indoor volume. The method is independent of viral load, droplet emission rate, and the dose-response relationship for a given virus and is based on the Wells-Riley model. The method estimates the maximum possible absolute difference $\Delta P_{abs.} = P_1 - P_2$ between infection risks before (P_1) and after (P_2) applying given control measures. For non-steady-state conditions, the method requires input information on the room volume, exposure time, inhalation rate, and removal rates before and after applying the infection control strategies. For steady-state conditions, the only input the model requires are the total removal rates before and after implementing control measures. We have demonstrated the application of the method for different viruses and infection control methods. We also showed that combining the different methods will not additively reduce the potential absolute risk reduction. The method offers decision-makers a more robust tool for creating safer and more cost-effective indoor environments.

CRediT authorship contribution statement

Amar Aganovic: Writing – original draft, Methodology, Investigation, Conceptualization. **Jarek Kurnitski:** Writing – review & editing, Methodology, Conceptualization. **Pawel Wargocki:** Writing – review & editing, Methodology, Conceptualization.

Declaration of competing interest

The authors declare that they have no known competing financial interests or personal relationships that could have appeared to influence the work reported in this paper.

Data availability

Data will be made available on request.

Acknowledgments

This work was supported by the Estonian Research Council grant (PRG2154), and by the Estonian Centre of Excellence in Energy Efficiency, ENER (grant TK230) funded by the Estonian Ministry of Education and Research. We would like to thank Prof. David P. Wyon for editing and proofreading the manuscript.

References

Aganovic, A., Kadric, E., 2023. Does the exponential Wells-Riley model provide a good fit for human coronavirus and rhinovirus? A comparison of four dose-response models based on human challenge data [published online ahead of print, 2023 Jun 15]. Risk Anal. https://doi.org/10.1111/risa.14178.

Aganovic, A., Bi, Y., Cao, G., Drangsholt, F., Kurnitski, J., Wargocki, P., 2021. Estimating the impact of indoor relative humidity on SARS-CoV-2 airborne transmission risk using a new modification of the Wells-Riley model. Build. Environ. 205, 108278 https://doi.org/10.1016/j.buildenv.2021.108278.

Aganovic A, Bi Y, Cao G, Kurnitski J, Wargocki P. Modeling the impact of indoor relative humidity on the infection risk of five respiratory airborne viruses. Sci. Rep. 2022a;12 (1):11481. Published 2022 Jul 7. doi:https://doi.org/10.1038/s41598-022-15703-8.

Aganovic, A., Bi, Y., Cao, G., Kurnitski, J., Wargocki, P., 2022b. Modeling the impact of indoor relative humidity on the infection risk of five respiratory airborne viruses. Sci. Rep. 12 (1), 11481. Published 2022 Jul 7. https://doi.org/10.1038/s41598-022-15703-8.

Aganovic, A., Cao, G., Kurnitski, J., Wargocki, P., 2023. New dose-response model and SARS-CoV-2 quanta emission rates for calculating the long-range airborne infection risk. Build. Environ. 228, 109924 https://doi.org/10.1016/j.buildenv.2022.109924.

ASHRAE Standard 241, 2023. Control of Infectious Aerosols. ASHRAE.

Batterman, S., 2017. Review and extension of CO_2-based methods to determine ventilation rates with application to school classrooms. Int. J. Environ. Res. Public Health 14(2):145. https://doi.org/10.3390/ijerph14020145. Published 2017 Feb 4.

Biasin, M., Bianco, A., Pareschi, G., et al., 2021. UV-C irradiation is highly effective in inactivating SARS-CoV-2 replication. Sci. Rep. 11(1):6260 https://doi.org/10.1038/s41598-021-85425-w. Published 2021 Mar 18.

Bourouiba, L., Dehandschoewercker, E., Bush, J.W.M., 2014. Violent expiratory events: on coughing and sneezing. J. Fluid Mech. 745, 537–563. https://doi.org/10.1017/jfm.2014.88.

Chatoutsidou, S.E., Lazaridis, M., 2019. Assessment of the impact of particulate dry deposition on soiling of indoor cultural heritage objects found in churches and museums/librariesJ. Cult. Heritage 39, 221–228. https://doi.org/10.1016/j.culher.2019.02.017.

Dabisch, P., Schuit, M., Herzog, A., et al., 2021. The influence of temperature, humidity, and simulated sunlight on the infectivity of SARS-CoV-2 in aerosols. Aerosol Sci. Technol. 55 (2), 142–153. https://doi.org/10.1080/02786826.2020.1829536.

Furlow, B., 2023. US CDC announces indoor air guidance for COVID-19 after 3 years. Lancet Respir. Med. 11 (7), 587. https://doi.org/10.1016/S2213-2600(23)00229-1.

Harmon, M., Lau, J., 2022. The Facility Infection Risk EstimatorTM: a web application tool for comparing indoor risk mitigation strategies by estimating airborne transmission risk. Indoor and Built Environment. 31 (5), 1339–1362. https://doi.org/10.1177/1420326X211039544.

Hodson, R., 2022. Preparing the world for the next pandemic. Nature 610 (7933), S33. https://doi.org/10.1038/d41586-022-03353-9.

Iddon, C., Jones, B., Sharpe, P., Cevik, M., Fitzgerald, S., 2022. A population framework for predicting the proportion of people infected by the far-field airborne transmission of SARS-CoV-2 indoors. Build. Environ. 221, 109309.

Izadyar, N., Miller, W., 2022. Ventilation strategies and design impacts on indoor airborne transmission: a review. Build. Environ. 218, 109158 https://doi.org/10.1016/j.buildenv.2022.109158.

Jones, B., Sharpe, P., Iddon, C., Hathway, E.A., Noakes, C.J., Fitzgerald, S., 2021. Modelling uncertainty in the relative risk of exposure to the SARS-CoV-2 virus by airborne aerosol transmission in well mixed indoor air. Build. Environ. 191, 107617 https://doi.org/10.1016/j.buildenv.2021.107617.

Jones, Benjamin and Iddon, Christopher and Sherman, Max Howard, Quantifying Quanta: Why We Can't Be Certain About the Risks of Long-range Airborne Infection. Available at SSRN: https://ssrn.com/abstract=4595141 or https://doi.org/10.2139/ssrn.4595141.

Kurnitski, J., Kiil, M., Mikola, A., Võsa, K.-V., Aganovic, A., Schild, P., Seppänen, O., 2023. Post-COVID ventilation design: infection risk-based target ventilation rates and point source ventilation effectiveness. Energ. Buildings 296, 113386. https://doi.org/10.1016/j.enbuild.2023.113386.

Lewis, D., 2022. Why the WHO took two years to say COVID is airborne. Nature 604 (7904), 26–31. https://doi.org/10.1038/d41586-022-00925-7.

Luo, B., Schaub, A., Glas, I., et al., 2023. Expiratory aerosol pH: the overlooked driver of airborne virus inactivation. Environ. Sci. Technol. 57 (1), 486–497. https://doi.org/10.1021/acs.est.2c05777.

Mariam, Magar A., Joshi, M., et al., 2021. CFD simulation of the airborne transmission of COVID-19 vectors emitted during respiratory mechanisms: revisiting the concept of safe distance. ACS Omega 6 (26), 16876–16889. Published 2021 Jun 23. https://doi.org/10.1021/acsomega.1c01489.

McDevitt, J., Rudnick, S., Radonovich, L., 2010. Characterization of UVC light sensitivity of influenza virus aerosols. In: AAAR 29th Annual Conference, p. 389.

A. Mikszewski, L. Stabile, G. Buonanno, L. Morawska. The Airborne Contagiousness of Respiratory Viruses: A Comparative Analysis and Implications for Mitigation. medRxiv 2021a.01.26.21250580. doi:https://doi.org/10.1101/2021.01.26.21250580.

Mikszewski, A., Stabile, L., Buonanno, G., Morawska, L., 2021b. The airborne contagiousness of respiratory viruses: a comparative analysis and implications for mitigation. Geosci. Front. 13 (6), 101285.

Morens, D.M., Park, J., Taubenberger, J.K., 2023. Many potential pathways to future pandemic influenza. Sci. Transl. Med. 15(718):eadj2379 https://doi.org/10.1126/scitranslmed.adj2379.

Motamedi, H., Shirzadi, M., Tominaga, Y., Mirzaei, P.A., 2022. CFD modeling of airborne pathogen transmission of COVID-19 in confined spaces under different ventilation strategies. Sustain. Cities Soc. 76, 103397 https://doi.org/10.1016/j.scs.2021.103397.

Nordic Ventilation Group, 2022. Rehva Technology and Research Committee COVID-19 Task ForceHealth-based target ventilation rates and design method for reducing exposure to airborne respiratory infectious diseases. REHVA proposal for post COVID target ventilation rates. Rehva.

de Oliveira, P.M., Mesquita, L.C.C., Gkantonas, S., Giusti, A., Mastorakos, E., 2021. Evolution of spray and aerosol from respiratory releases: theoretical estimates for insight on viral transmission. Proc Math Phys Eng Sci. 477 (2245), 20200584. https://doi.org/10.1098/rspa.2020.0584.

Peng, Z., Jimenez, J.L., 2021. Exhaled CO_2 as a COVID-19 infection risk proxy for different indoor environments and activities. Environ. Sci. Technol. Lett. 8, 392–397.

Peng, Z., Rojas, A.L.P., Kropff, E., et al., 2022. Practical indicators for risk of airborne transmission in shared indoor environments and their application to COVID-19 outbreaks [published correction appears in Environ Sci Technol. 2022 Mar 1;56(5): 3302-3303]. Environ. Sci. Technol. 56 (2), 1125–1137. https://doi.org/10.1021/acs.est.1c06531.

Rayegan, S., Shu, C., Berquist, J., et al., 2023. A review on indoor airborne transmission of COVID-19– modelling and mitigation approaches. Journal of Building Engineering. 64, 105599 https://doi.org/10.1016/j.jobe.2022.105599.

Sze To GN, Chao, C.Y., 2010. Review and comparison between the Wells-Riley and dose-response approaches to risk assessment of infectious respiratory diseases. Indoor Air 20 (1), 2–16. https://doi.org/10.1111/j.1600-0668.2009.00621.x.

Tan, H., Wong, K.Y., Othman, M.H.D., Kek, H.Y., Nyakuma, B.B., Ho, W.S., Hashim, H., Wahab, R.A., Sheng, D.D.C.V., Wahab, N.H.A., Yatim, A.S., 2023. Why do ventilation strategies matter in controlling infectious airborne particles? A comprehensive numerical analysis in isolation ward. Build. Environ. 231 (Article 110048).

The Lancet COVID-19 Commission Task Force on Safe Work, Safe School, and Safe Travel, 2023. Proposed Non-infectious Air Delivery Rates (NADR) for Reducing Exposure to Airborne Respiratory Infectious Diseases.

Wang, C.C., Prather, K.A., Sznitman, J., et al., 2021. Airborne transmission of respiratory viruses. Science 373(6558):eabd9149. https://doi.org/10.1126/science.abd9149.

Watanabe, T., Bartrand, T.A., Weir, M.H., Omura, T., Haas, C.N., 2010. Development of a dose-response model for SARS coronavirus. Risk Anal. 30 (7), 1129–1138. https://doi.org/10.1111/j.1539-6924.2010.01427.x.

WHO. vol. 38. 2021. Roadmap to improve and ensure good indoor ventilation in the context of COVID-19. https://www.who.int/publications/i/item/9789240021280.

Xie, X., Li, Y., Chwang, A.T.Y., Ho, P.L., Seto, W.H., 2007. How far droplets can move in indoor environments? Revisiting the Wells evaporation-falling curve. Indoor Air 17, 211–225. https://doi.org/10.1111/j.1600-0668.2007.00469.x.